

# Supporting Information

## Charge Transport Network Dynamics in Molecular Aggregates

Nicholas E. Jackson<sup>1</sup>, Lin X. Chen<sup>1,2</sup>, Mark A. Ratner<sup>1</sup>

<sup>1</sup>Department of Chemistry, Northwestern University, 2145  
Sheridan Rd., Evanston, Illinois 60208, United States.

<sup>2</sup> Chemical Sciences and Engineering Division, Argonne National Laboratory,  
Lemont, Illinois 60439, United States

### Table of Contents:

1. Simulation Box Protocols
2. OPLS Force-Field Parameters
3. Relevant Input Files for LAMMPS
4. Figure 3 Fits
5. Transfer Integral TCF & Fourier Transform
6. TCF of Matrix Spectral Norm
7. Correlations between Kirchoff Index and Zero-Field Mobilities Using a Kinetic Monte Carlo Model

### Simulation Box Protocol

Since this manuscript is primarily concerned with network methodological development for analyzing amorphous systems, our simulation procedure is not overly concerned with identifying the lowest energy non-crystalline morphology possible. If this were the case, a longer (~microseconds) and more gradual morphology simulation would be required. However, for the purposes of our short-time electronic dynamics (~20 ps), the following procedure is sufficient for generating a morphology required for electronic structure analysis.

### **Disordered PDI**

1. A cubic box of length 100 Angstroms was randomly packed with 64 PDI molecules possessing random locations and orientations.
2. A force minimization is done in combination with a box compression to increase the density of the initially diffusely packed box, while simultaneously removing any bad contacts. This is followed by a brief (<20 ps) NVE run to reinitialize the packing of the box.
3. Another force minimization with box compression is performed to further compress the box to within a factor of 2 of the expected density. This is once again followed by a brief 20 ps NVE re-initialization of the box geometry.

4. A 100 ps NPT heating run is performed at 1 atm from 10K to 550K, the annealing temperature. The velocity distribution is randomly initialized according to the Boltzmann distribution.
5. A 10 ns NPT annealing run at 550K
6. A 10 ns NPT cooling run from 550K to 298 K.
7. A 10 ns NPT equilibration run at 298K.
8. A 1 ns NVT equilibration run at the average box volume of the previous 10 ns run.
9. A 100 ps NVE equilibration.
10. A 20 ps NVE sampling run, where the data in the manuscript is taken at 10 fs intervals.

### **Disordered bBDT(TDPP)<sub>2</sub>**

11. A cubic box of length 100 Angstroms was randomly packed with 100 BTI molecules possessing random locations and orientations.
12. A force minimization is done in combination with a box compression to increase the density of the initially diffusely packed box, while simultaneously removing any bad contacts. This is followed by a brief (<20 ps) NVE run to reinitialize the packing of the box.
13. Another force minimization with box compression is performed to further compress the box to within a factor of 2 of the expected density. This is once again followed by a brief 20 ps NVE re-initialization of the box geometry.
14. A 100 ps NPT heating run is performed at 1 atm from 10K to 550K, the annealing temperature. The velocity distribution is randomly initialized according to the Boltzmann distribution.
15. A 10 ns NPT annealing run at 550K
16. A 10 ns NPT cooling run from 550K to 298 K.
17. A 10 ns NPT equilibration run at 298K.
18. A 1 ns NVT equilibration run at the average box volume of the previous 10 ns run.
19. A 100 ps NVE equilibration.
20. A 20 ps NVE sampling run, where the data in the manuscript is taken at 10 fs intervals.

### **Crystalline bBDT(TDPP)<sub>2</sub>**

21. The unit cell of bBDT(TDPP)<sub>2w</sub> was repeated in a 5x5x2 block composed of 100 molecules, and a simulation cell corresponding to the appropriate unit cell was constructed.
22. A force minimization is done to remove bad contacts. This is followed by a brief (<20 ps) NVE run to reinitialize the packing of the box.
23. A 100 ps NPT heating run is performed at 1 atm from 10K to 550K, the annealing temperature. The velocity distribution is randomly initialized according to the Boltzmann distribution.

24. A 10 ns NPT annealing run at 550K
25. A 10 ns NPT cooling run from 550K to 298 K.
26. A 10 ns NPT equilibration run at 298K.
27. A 1 ns NVT equilibration run at the average box volume of the previous 10 ns run.
28. A 100 ps NVE equilibration.
29. A 20 ps NVE sampling run, where the data in the manuscript is taken at 10 fs intervals.

### OPLS Force-Field Parameters

Since standard OPLS force-field parameters do not accurately describe the atomic geometry, atomic partial charges, and dihedral angles of PDI and bBDT(TDPP)<sub>2</sub>, many of these values were parameterized by hand using quantum-chemical calculations. All bond distances and angle values were taken from the B3LYP/6-31G\*\* geometry optimized structures. Atomic partial charges were determined by performing B3LYP/6-31G\*\* CHelpG calculations on the geometry optimized structure. Improper dihedral angles were selected to rigidify the pi-system. The specific OPLS2009 parameters provided below are taken from the TINKER .prm files, as they are presented in an easily digestible format.

#### PDI

```

atom    907  110 N "PDI N1 class 35" 7 14.007 3
atom    908   111 C "PDI C2 class 3" 6 12.011 3
atom    909   112 C "PDI C3 class 38" 6 12.011 3
atom    910   113 C "PDI C4 class 38" 6 12.011 3
atom    911   114 C "PDI C5 class 38" 6 12.011   3
atom    912   115 C "PDI C6 class 38" 6 12.011   3
atom    913   116 C "PDI C7 class 38" 6 12.011 3
atom    914   117 C "PDI C8 class 38" 6 12.011 3
atom    915   118 O "PDI O9 class 4" 8 15.999 1
atom    916    13 C "PDI C10 class 13" 6 12.011 4
atom    917    39 H "PDI H11 class 39" 1 1.008 1
atom    918    39 H "PDI H12 class 39" 1 1.008 1
bond    110   111 490.00 1.409
bond    110    13 337.00 1.497
bond    111   112 400.00 1.484
bond    112   113 469.00 1.385
bond    113   114 469.00 1.399
bond    114   115 469.00 1.396
bond    115   116 469.00 1.431
bond    116   117 469.00 1.429
bond    111   118 570.00 1.225
bond    115   115 469.00 1.470
bond    112   117 469.00 1.414
bond    113    39 367.00 1.083
bond    114    39 367.00 1.083
angle   111   110   111 70.00 123.8
angle   111   110    13 50.00 117.0
angle   110   111   112 70.00 117.3
angle   110   111   118 80.00 121.4
angle   112   111   118 80.00 121.3
angle   111   112   113 85.00 119.3
angle   111   112   117 85.00 121.1
angle   113   112   117 63.00 119.6

```

angle	112	113	114	63.00	120.4								
angle	112	113	39	35.00	118.7								
angle	114	113	39	35.00	120.9								
angle	113	114	115	63.00	121.9								
angle	113	114	39	35.00	117.8								
angle	115	114	39	35.00	120.2								
angle	114	115	115	63.00	122.4								
angle	114	115	116	63.00	118.5								
angle	115	115	116	63.00	119.1								
angle	115	116	115	63.00	121.8								
angle	115	116	117	63.00	119.1								
angle	112	117	112	63.00	119.3								
angle	112	117	116	63.00	120.4								
angle	110	13	13	80.00	111.7								
angle	110	13	36	35.00	103.1								
torsion	111	110	111	112	0.000	0.0	1	7.250	180.0	2	0.000	0.0	3
torsion	111	110	111	118	0.000	0.0	1	2.100	180.0	2	0.000	0.0	3
torsion	13	110	111	112	0.000	0.0	1	7.250	180.0	2	0.000	0.0	3
torsion	13	110	111	118	0.000	0.0	1	2.100	180.0	2	0.000	0.0	3
#side-chain torsion													
torsion	111	110	13	13	0.000	0.0	1	0.000	180.0	2	0.000	0.0	3
torsion	111	110	13	36	0.000	0.0	1	0.000	180.0	2	0.000	0.0	3
torsion	110	111	112	113	0.000	0.0	1	7.250	180.0	2	0.000	0.0	3
torsion	110	111	112	117	0.000	0.0	1	7.250	180.0	2	0.000	0.0	3
torsion	118	111	112	113	0.000	0.0	1	2.100	180.0	2	0.000	0.0	3
torsion	118	111	112	117	0.000	0.0	1	2.100	180.0	2	0.000	0.0	3
torsion	111	112	113	114	0.000	0.0	1	7.250	180.0	2	0.000	0.0	3
torsion	111	112	113	39	0.000	0.0	1	7.250	180.0	2	0.000	0.0	3
torsion	117	112	113	39	0.000	0.0	1	7.250	180.0	2	0.000	0.0	3
torsion	111	112	117	112	0.000	0.0	1	7.250	180.0	2	0.000	0.0	3
torsion	111	112	117	116	0.000	0.0	1	7.250	180.0	2	0.000	0.0	3
torsion	117	112	113	114	0.000	0.0	1	7.250	180.0	2	0.000	0.0	3
torsion	113	112	117	112	0.000	0.0	1	7.250	180.0	2	0.000	0.0	3
torsion	113	112	117	116	0.000	0.0	1	7.250	180.0	2	0.000	0.0	3
torsion	112	113	114	115	0.000	0.0	1	7.250	180.0	2	0.000	0.0	3
torsion	112	113	114	39	0.000	0.0	1	7.250	180.0	2	0.000	0.0	3
torsion	39	113	114	115	0.000	0.0	1	7.250	180.0	2	0.000	0.0	3
torsion	39	113	113	39	0.000	0.0	1	7.250	180.0	2	0.000	0.0	3
torsion	39	113	114	39	0.000	0.0	1	7.250	180.0	2	0.000	0.0	3
torsion	113	114	115	115	0.000	0.0	1	7.250	180.0	2	0.000	0.0	3
torsion	113	114	115	116	0.000	0.0	1	7.250	180.0	2	0.000	0.0	3
torsion	39	114	115	115	0.000	0.0	1	7.250	180.0	2	0.000	0.0	3
torsion	39	114	115	116	0.000	0.0	1	7.250	180.0	2	0.000	0.0	3
torsion	114	115	115	114	0.000	0.0	1	7.250	180.0	2	0.000	0.0	3
torsion	114	115	115	116	0.000	0.0	1	7.250	180.0	2	0.000	0.0	3
torsion	114	115	116	117	0.000	0.0	1	7.250	180.0	2	0.000	0.0	3
torsion	116	115	115	116	0.000	0.0	1	7.250	180.0	2	0.000	0.0	3
torsion	114	115	116	115	0.000	0.0	1	7.250	180.0	2	0.000	0.0	3
torsion	115	115	116	115	0.000	0.0	1	7.250	180.0	2	0.000	0.0	3
torsion	115	115	116	117	0.000	0.0	1	7.250	180.0	2	0.000	0.0	3
torsion	115	116	117	112	0.000	0.0	1	7.250	180.0	2	0.000	0.0	3
torsion	110	13	13	13	0.845	0.0	1	-0.962	180.0	2	0.713	0.0	3
torsion	110	13	13	36	0.000	0.0	1	0.000	180.0	2	0.464	0.0	3
charge	907	-0.148											
charge	908	0.534											
charge	909	-0.270											
charge	910	0.010											
charge	911	-0.220											
charge	912	0.060											
charge	913	0.050											
charge	914	0.210											
charge	915	-0.480											
charge	916	0.040											
charge	917	0.120											
charge	918	0.140											
vdw	907	3.2500	0.1700										
vdw	908	3.7500	0.1050										
vdw	909	3.5500	0.0700										
vdw	910	3.5500	0.0700										

vdw	911	3.5500	0.0700						
vdw	912	3.5500	0.0700						
vdw	913	3.5500	0.0700						
vdw	914	3.5500	0.0700						
vdw	915	2.9600	0.2100						
vdw	916	3.5000	0.0660						
vdw	917	2.4200	0.0300						
vdw	918	2.4200	0.0300						
torsion	3 35 3 38	0.000	0.0 1	7.250	180.0 2		0.000	0.0 3	
torsion	3 35 3 4		0.000	0.0 1	7.250	180.0 2		0.000	0.0 3
torsion	13 35 3 38		0.000	0.0 1	0.000	180.0 2		0.000	0.0 3
imptors	111 112 113 114	0.000		0.0 1	0.001	180.0 2		0.000	0.0 3
imptors	0 0 111 118	0.000	0.0 1	7.250	180.0 2		0.000	0.0 3	

## bBDT(TDPP)<sub>2</sub>

atom	907	101 S	"Thiophene1 S"	16	32.060	2			
atom	908	102 Cd	"Thiophene1 C2"	6	12.011	3			
atom	909	103 CS	"Thiophene1 C3"	6	12.011	3			
atom	910	104 CS	"Thiophene1 C4"	6	12.011	3			
atom	911	105 Cd	"Thiophene1 C5"	6	12.011	3			
atom	912	106 HA	"Thiophene1 H1"	1	1.008	1			
charge	907		0.03						
charge	908		-0.18						
charge	909		-0.17						
charge	910		-0.12						
charge	911		0.03						
charge	912		0.16						
vdw	907	3.5500	0.2500						
vdw	908	3.5500	0.0700						
vdw	909	3.5500	0.0700						
vdw	910	3.5500	0.0700						
vdw	911	3.5500	0.0700						
vdw	912	2.4200	0.0300						
atom	913	107 NA	"diKetoPyrrole N"	7	14.007	3			
atom	914	108 CW	"diKetoPyrrole C2O"	6	12.011	3			
atom	915	109 CW	"diKetoPyrrole C3"	6	12.011	3			
atom	916	110 CN	"diKetoPyrrole C4"	6	12.011	3			
atom	917	111 O	"diKetoPyrrole C=O"	8	15.999	1			
atom	918	13 CT	"diKetoPyrrole SC-CH2"	6	12.011	4			
charge	913		-0.21						
charge	914		0.50						
charge	915		0.12						
charge	916		-0.25						
charge	917		-0.50						
charge	918		0.10						
vdw	913	3.2500	0.1700						
vdw	914	3.5500	0.0700						
vdw	915	3.5500	0.0700						
vdw	916	3.5500	0.0700						

vdw	917	2.9600	0.2100
vdw	918	3.5500	0.0700
atom	919	101 S "Thiophene2 S" 16 32.060 2	
atom	920	102 Cd "Thiophene2 C2" 6 12.011 3	
atom	921	103 CS "Thiophene2 C3" 6 12.011 3	
atom	922	104 CS "Thiophene2 C4" 6 12.011 3	
atom	923	105 Cd "Thiophene2 C5" 6 12.011 3	
atom	924	106 HA "Thiophene2 H1" 1 1.008 1	
charge	919	-0.10	
charge	920	0.12	
charge	921	-0.26	
charge	922	-0.15	
charge	923	0.13	
charge	924	0.16	
vdw	919	3.5500	0.2500
vdw	920	3.5500	0.0700
vdw	921	3.5500	0.0700
vdw	922	3.5500	0.0700
vdw	923	3.5500	0.0700
vdw	924	2.4200	0.0300
atom	925	112 S "BDT S" 16 32.060 2	
atom	926	113 C "BDT C1" 6 12.011 3	
atom	927	114 C "BDT C2" 6 12.011 3	
atom	928	115 C "BDT C3" 6 12.011 3	
atom	929	116 C "BDT C4" 6 12.011 3	
atom	930	117 C "BDT C5" 6 12.011 3	
atom	931	118 C "BDT SC C6" 6 12.011 4	
atom	932	119 HA "BDT H1" 1 1.008 1	
charge	925	-0.03	
charge	926	-0.10	
charge	927	-0.120001	
charge	928	0.000001	
charge	929	0.05	
charge	930	-0.10	
charge	931	0.10	
charge	932	0.19	
vdw	925	3.5500	0.2500
vdw	926	3.5500	0.0700
vdw	927	3.5500	0.0700
vdw	928	3.5500	0.0700
vdw	929	3.5500	0.0700
vdw	930	3.5500	0.0700
vdw	931	3.5500	0.0700
vdw	932	2.4200	0.0300
#thio1			
bond	101 102	250.00	1.727

bond	102	103	546.00	1.371	
bond	103	104	546.00	1.416	
bond	104	105	546.00	1.389	
bond	105	101	250.00	1.764	
bond	102	106	367.00	1.08	
bond	103	106	367.00	1.08	
bond	104	106	367.00	1.08	
bond	109	102	546.00	1.440	
angle	102	101	105	74.00	91.8
angle	101	102	103	70.00	111.9
angle	101	102	106	35.00	119.6
angle	103	102	106	35.00	128.5
angle	102	103	104	70.00	113.1
angle	102	103	106	35.00	123.4
angle	104	103	106	35.00	123.6
angle	103	104	105	70.00	113.5
angle	103	104	106	35.00	124.6
angle	105	104	106	35.00	121.9
angle	101	105	104	70.00	109.7
#DPP					
bond	105	109	546.00	1.442	
bond	107	108	427.00	1.434	
bond	107	109	427.00	1.395	
bond	108	110	546.00	1.445	
bond	109	110	546.00	1.398	
bond	110	110	546.00	1.420	
bond	108	111	570.00	1.230	
bond	107	13	337.00	1.461	
angle	101	105	109	70.00	105.9
angle	104	105	109	70.00	124.4
angle	108	107	109	64.00	111.5
angle	108	107	13	70.00	118.4
angle	109	107	13	70.00	130.1
angle	107	108	110	70.00	104.2
angle	107	108	111	80.00	122.2
angle	110	108	111	80.00	133.6
angle	107	109	102	70.00	127.1
angle	107	109	110	70.00	106.6
angle	110	109	102	70.00	126.3
angle	105	109	107	70.00	127.0
angle	105	109	110	70.00	126.3
angle	108	110	109	70.00	142.3
angle	108	110	110	70.00	108.2
angle	109	110	110	70.00	109.5
angle	107	13	13	58.35	113.0
angle	107	13	36	35.00	107.0

```

angle    109    102 101 70.00 125.9
angle    109    102 103 70.00 125.8
#BDT
bond     105    113 546.00 1.441
bond     112    113 250.00 1.771
bond     113    114 546.00 1.373
bond     114    115 546.00 1.432
bond     115    116 546.00 1.414
bond     116    112 250.00 1.751
bond     116    116 546.00 1.393
bond     115    117 546.00 1.432
bond     117    118 469.00 1.518
bond     117    117 546.00 1.395
bond     114    119 367.00 1.080
bond     118     13 367.00 1.080
bond     118     36 268.00 1.529
angle    101    105 113 70.00 120.9
angle    104    105 113 70.00 128.8
angle    113    112 116 74.00 90.9
angle    105    113 112 70.00 119.9
angle    105    113 114 70.00 128.7
angle    112    113 114 70.00 111.3
angle    113    114 115 70.00 114.5
angle    113    114 119 35.00 125.9
angle    115    114 119 35.00 123.6
angle    114    115 116 70.00 111.0
angle    114    115 117 70.00 128.0
angle    116    115 117 70.00 121.0
angle    112    116 115 70.00 112.3
angle    112    116 116 70.00 128.3
angle    115    116 116 70.00 119.7
angle    115    117 117 70.00 119.2
angle    115    117 118 70.00 117.6
angle    117    117 118 70.00 123.2
angle    117    118 36 35.00 107.0
angle     13    118 36 35.00 107.0
angle    118 13 13 58.35 113.0
angle    118     13 36 35.00 107.0
angle    117    117 13 70.00 123.2
angle     36    118 36 33.00 107.8
angle    117 118 13 58.35 112.7
#torsion
torsion   0 103 104 0 0.000 0.0 1 7.250 180.0 2 0.000 0.0 3 0.000 180.0 4
torsion   0 102 103 0 0.000 0.0 1 7.250 180.0 2 0.000 0.0 3 0.000 180.0 4
torsion   0 101 102 0 0.000 0.0 1 7.250 180.0 2 0.000 0.0 3 0.000 180.0 4
torsion   0 101 105 0 0.000 0.0 1 7.250 180.0 2 0.000 0.0 3 0.000 180.0 4

```



```

torsion    0 104 105  0   0.000 0.0 1 7.250 180.0 2 0.000 0.0 3 0.000 180.0 4
torsion    0 101 102  0   0.000 0.0 1 7.250 180.0 2 0.000 0.0 3 0.000 180.0 4
#DIHEDRAL THIO 1
torsion    101   105 109 107   0.000 0.0 1 0.000 180.0 2 0.000 0.0 3 0.000   180.0 4
torsion    104   105 109 107   0.000 0.0 1 0.000 180.0 2 0.000 0.0 3 0.000   180.0 4
#torsion   104   105 109 110   -2.017 0.0 1 8.394 180.0 2 -1.725 0.0 3 0.151   180.0 4
torsion   104 105 109 110 -1.906 0.0 1 8.514 180.0 2 -1.613 0.0 3 0.271 180.0 4
torsion    101   105 109 110   0.000 0.0 1 0.000 180.0 2 0.000 0.0 3 0.000   180.0 4
#
torsion    0   107 108  0   0.000 0.0 1 7.250 180.0 2 0.000 0.0 3 0.000   180.0 4
torsion    0 107 109  0   0.000 0.0 1 7.250 180.0 2 0.000 0.0 3 0.000   180.0 4
torsion    0   107 13 13   1.000 0.0 1 -0.350 180.0 2 0.000 0.0 3 0.000   180.0 4
torsion    0 13 13 107   0.000 0.0 1 0.000 180.0 2 0.462 0.0 3 0.000   180.0 4
torsion    0   107 13 36   0.000 0.0 1 0.000 180.0 2 0.000 0.0 3 0.000   180.0 4
torsion    0   108 110  0   0.000 0.0 1 10.750 180.0 2 0.000 0.0 3
torsion    0   110 110  0   0.000 0.0 1 10.750 180.0 2 0.000 0.0 3
torsion    0   109 110  0   0.000 0.0 1 10.750 180.0 2 0.000 0.0 3
#DIHEDRAL THIO 2
torsion    107   109 102 101 0.000 0.0 1 0.000 180.0 2 0.000 0.0 3
torsion    107   109 102 103 0.000 0.0 1 0.000 180.0 2 0.000 0.0 3
torsion    110   109 102 101 0.000 0.0 1 0.000 180.0 2 0.000 0.0 3
torsion    110   109 102 103 -2.100 0.0 1 8.536 180.0 2 -1.840 0.0 3 -0.009 180.0 4
#
#DIHEDRAL 3 THIO-BDT
torsion    101   105 113 112   0.000 0.0 1 0.000 180.0 2 0.000 0.0 3
torsion    101   105 113 114   0.133 0.0 1 2.754 180.0 2 -0.195 0.0 3 -1.011 180.0 4
torsion    104   105 113 112   0.000 0.0 1 0.000 180.0 2 0.000 0.0 3
torsion    104   105 113 114   0.000 0.0 1 0.000 180.0 2 0.000 0.0 3
#
torsion    0 112 113  0 0.000 0.0 1 7.250 180.0 2 0.000 0.0 3
torsion    0   112 116  0   0.000 0.0 1 7.250 180.0 2 0.000 0.0 3
torsion    0   113 114  0   0.000 0.0 1 7.250 180.0 2 0.000 0.0 3
torsion    0   114 115  0   0.000 0.0 1 7.250 180.0 2 0.000 0.0 3
torsion    0   115 116  0   0.000 0.0 1 7.250 180.0 2 0.000 0.0 3
torsion    0   115 117  0   0.000 0.0 1 7.250 180.0 2 0.000 0.0 3
torsion    0   116 116  0   0.000 0.0 1 7.250 180.0 2 0.000 0.0 3
torsion    0   117 117  0   0.000 0.0 1 7.250 180.0 2 0.000 0.0 3
torsion    0   117 118 13   0.000 0.0 1 0.000 180.0 2 0.000 0.0 3
torsion    0   117 118 36   0.000 0.0 1 0.000 180.0 2 0.000 0.0 3
torsion    0   118 13 13   1.000 0.0 1 -0.350 180.0 2 0.000 0.0 3
torsion    118   13 13 13   1.300 0.0 1 -0.050 180.0 2 0.000 0.0 3
torsion    118   13 13 36   0.000 0.0 1 0.000 180.0 2 0.300 0.0 3
torsion    36   118 13 36   0.000 0.0 1 0.000 180.0 2 0.300 0.0 3
torsion    117   118 13 36   0.000 0.0 1 0.000 180.0 2 0.000 0.0 3
#these parameters are just for refitting purposes
bond 109 106 367.0 1.08

```

```

bond 116 13 545.0 1.51
bond 113 106 367.0 1.08
bond 117 13 545.0 1.51
angle 110 109 106 35.00 130.4
angle 106 109 107 35.00 120.9
angle 115 117 13 70.00 120.5
angle 114 113 106 35.00 127.7
angle 106 113 112 70.00 119.3
angle 117 13 36 35.00 112.5
torsion 115 117 13 36 0.000 0.0 1 0.000 180.0 2 0.000 0.0 3
torsion 117 117 13 36 0.000 0.0 1 0.000 180.0 2 0.000 0.0 3
imptors 0 0 110 0 0.000 0.0 1 5.000 180.0 2 0.000 0.0 3

```

## Example Input File for Disordered PDI

### Control file

```

# ----- Init Section -----
include "box_of_PDI_label_min.in.init"

# ----- Atom Definition Section -----
read_data "box_of_PDI_label_min.data"

# ----- Setting Section -----
include "box_of_PDI_label_min.in.settings"

# ----- Run Section -----

#USING RATTLE TO GET TIMESTEP OF 2
thermo 1000
thermo_style custom step dt temp press vol etotal ke pe ebond eangle edihed eimp evdwl ecolong density
neigh_modify delay 0 every 1 check yes page 1000000 one 100000
run_style verlet

#QUICK COMPRESS TO CLEAN UP THE SIMULATION BOX
dump 1 all atom 1000 min.dump
fix 1 all box/relax iso 10000000.0 vmax 0.01
minimize 1.0e-6 1.0e-6 20000 200000
unfix 1
undump 1

#NVE EQUILIBRATION RUN (20 ps)
timestep 1
fix 2 all nve/limit 0.01
run 20000
unfix 2

#Second Compression Minimization
fix 3 all box/relax iso 10000000.0 vmax 0.01
minimize 1.0e-6 1.0e-6 20000 200000
unfix 3

#Second NVE Equil
timestep 1
fix 4 all nve/limit 0.01
run 20000
unfix 4

```

```

#Heating up
timestep 2
neigh_modify delay 5 every 1 check yes page 1000000 one 100000
fix 5 all npt temp 10.0 550.0 100.0 iso 1.0 1.0 1000
fix 15 all rattle 0.0001 20 0 m 1.008
run 50000
unfix 15
unfix 5

```

```

#ANNEALING RUN (550K for 2 ns)
fix 6 all npt temp 550.0 550.0 100.0 iso 1.0 1.0 1000
fix 16 all rattle 0.0001 20 0 m 1.008
run 5000000
unfix 16
unfix 6

```

```

#COOLING (550K - 298K over 100 ps)
fix 7 all npt temp 550.0 298.0 100 iso 1.0 1.0 1000
fix 17 all rattle 0.0001 20 0 m 1.008
run 5000000
unfix 17
unfix 7

```

```

#SIMULATION (nPT for 6 ns; 1 ns snapshots)
dump 8 all atom 1000000 equil.dump
fix 8 all npt temp 298.0 298.0 100 iso 1.0 1.0 1000
fix 18 all rattle 0.0001 20 0 m 1.008
run 5000000
unfix 18
unfix 8
undump 8

```

```

#NVT Run (nVT for 2 ns)
fix 200 all nvt temp 298.0 298.0 100
fix 201 all rattle 0.0001 20 0 m 1.008
run 500000
unfix 201
unfix 200

```

```

#NVE Equil
timestep 1
fix 700 all nve
run 50000
unfix 700

```

```

#SAMPLING (NVE for 20 ps; 10 fs snapshots)
timestep 1
dump 100 all atom 10 sample.dump
fix 100 all nve
run 20000
unfix 100
undump 100

```

```

#END OF RUN SECTION #

```

## **.init file**

```

units      real      # angstroms,kCal/mol,Daltons,Kelvin
atom_style full      # select column format for Atoms section
pair_style lj/cut/coul/long 10.0 10.0 # cutoffLJ cutoff_coulomb
bond_style harmonic #parameters needed: k_bond, r0
angle_style harmonic #parameters needed: k_theta, theta0
dihedral_style opls
improper_style cvff
kspace_style pppm 0.0001 # long-range electrostatics sum method
pair_modify mix arithmetic #using Lorenz-Berthelot mixing rules

```

## Simulation Details

The data of Figure 3 was fit using the `Optimize.curve_fit` routine in Scipy. This routine employ a non-linear least squares to fit a function,  $f$ , to the data. The data was fit to the form:

$$\text{TCF}(t) = A1 \cdot \exp(-b1 \cdot t) + A2 \cdot \exp(-b2 \cdot t)$$

The optimal values of the fitting parameters were the following:

### **Disordered PDI**

A1, A2, b1, b2

```
[ 0.49960115  0.48670783  0.00526324  0.03193688]
```

and the covariance matrix was:

```
[[ 9.02869987e-05 -7.80417345e-05  6.92676478e-07  8.72171357e-06]
 [ -7.80417345e-05  9.45332078e-05 -6.16078009e-07 -5.73017840e-06]
 [ 6.92676478e-07 -6.16078009e-07  6.30505437e-09  6.06600711e-08]
 [ 8.72171357e-06 -5.73017840e-06  6.06600711e-08  1.19407013e-06]]
```

### **Disordered bBDT(TDPP)<sub>2</sub>**

A1, A2, b1, b2

```
[ 0.4235485  0.57582765  0.18934241  0.01063638]
```

and the covariance matrix was:

```
[[ 2.11630386e-04 -1.10262518e-04 -1.17334933e-04 -1.89822556e-06]
 [ -1.10262518e-04  1.11650354e-04  1.42336942e-04  1.91805797e-06]
 [ -1.17334933e-04  1.42336942e-04  4.19904609e-04  2.24795900e-06]
 [ -1.89822556e-06  1.91805797e-06  2.24795900e-06  4.80374715e-08]]
```

### **Crystalline bBDT(TDPP)<sub>2</sub>**

A1, A2, b1, b2

```
[ 0.80770858  0.14074453  0.01317332  0.00311807]
```

and the covariance matrix was:

```
[[ 3.77322746e-04 -3.76912356e-04 -6.12503629e-06 -5.15227374e-06]
 [ -3.76912356e-04  4.25922587e-04  7.81860648e-06  5.69374574e-06]
 [ -6.12503629e-06  7.81860648e-06  1.76896233e-07  9.63502632e-08]
 [ -5.15227374e-06  5.69374574e-06  9.63502632e-08  8.46924134e-08]]
```

### **Local TCF Fourier Transform**

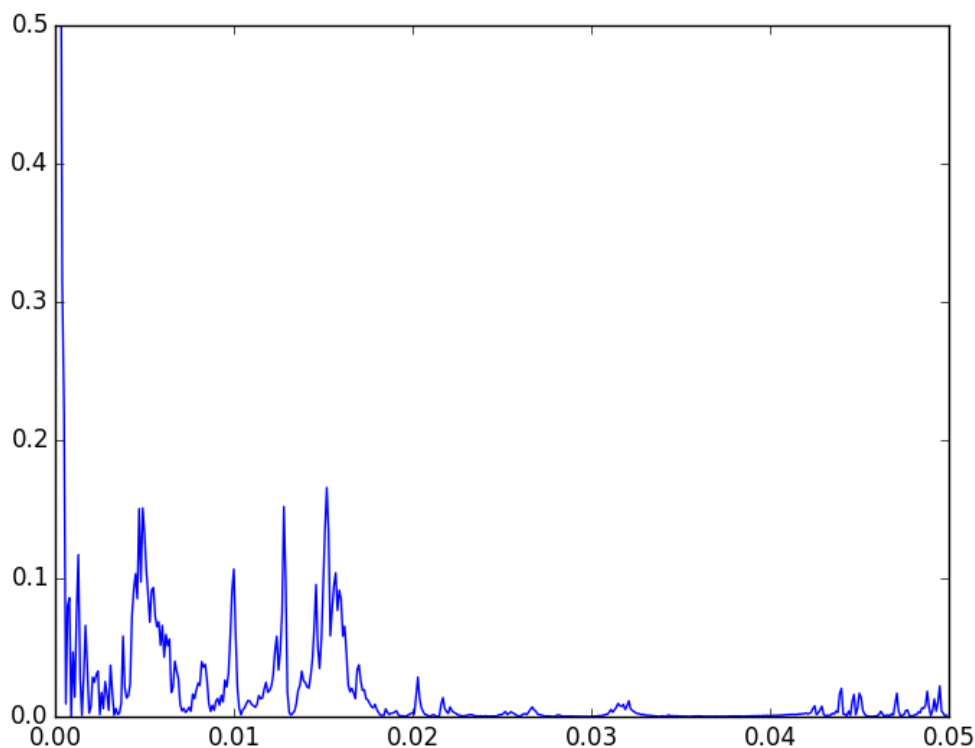


Figure S1 – Fourier spectrum of the ensemble averaged time-correlation function of the intermolecular electronic coupling between PDI LUMO's.

### **TCF of Matrix Spectral Norm**

To quantify how the self-similarity of the graph representing the charge transport network of the molecular aggregate evolves as a function of time, we compute a time-correlation function of the adjacency matrix spectral norm defined below. TCF reveals a decorrelation timescale of  $\sim 100$  fs, in agreement with the qualitative assignments derived from visual inspection of Figure 2 in the manuscript.

$$C_{ij}(\tau) = \lim_{T \rightarrow \infty} \int_0^T \frac{\text{SpecNorm}[A(t) - A(t + \tau)]}{T} dt$$

Where Norm represents the spectral norm, and A is the adjacency matrix at time t. The Spectral Norm TCF for all 5 trajectories are shown below.

PDI - Trajectory 1

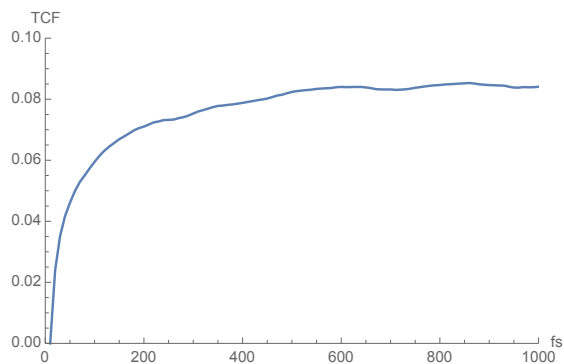


Figure S2 – TCF of the spectral norm of the adjacency matrix for PDI trajectory # 1.

PDI - Trajectory 2

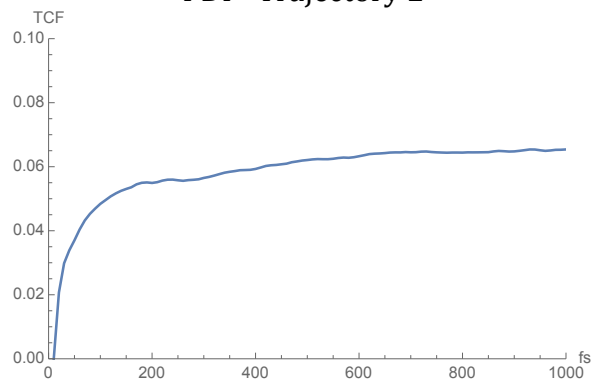


Figure S3 – TCF of the spectral norm of the adjacency matrix for PDI trajectory # 2.

### PDI - Trajectory 3

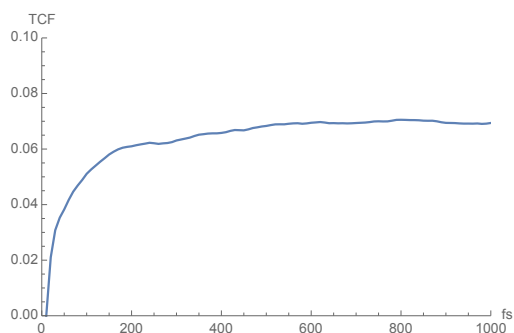


Figure S4 – TCF of the spectral norm of the adjacency matrix for PDI trajectory # 3.

### PDI - Trajectory 4

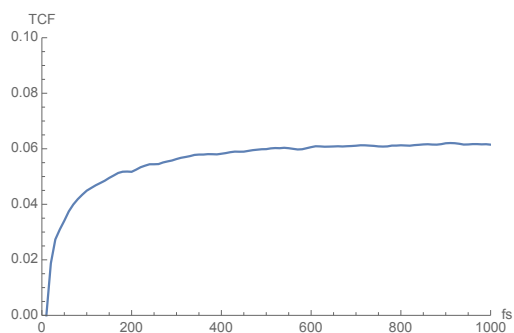


Figure S5 – TCF of the spectral norm of the adjacency matrix for PDI trajectory # 4.

### PDI - Trajectory 5

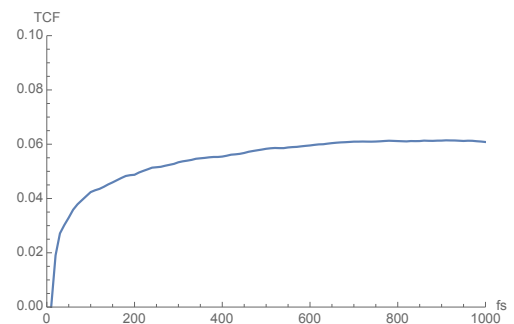


Figure S6 – TCF of the spectral norm of the adjacency matrix for PDI trajectory # 5.

## **Correlations between Kirchoff Index and Zero-Field Mobilities Using a Kinetic Monte Carlo Model**

While the correlation between the Kirchoff Index and experimental mobilities or diffusion constants has only been qualitative in previous work (Jackson – JPCL – 2015 – 1:1018-1021), here we use the same geometric model as in our previous work to generate example morphologies. Details on the description of the method for generating morphologies and the lattice model used can be found in our previous JPCL manuscript. These morphologies are then used to generate a realistic ensemble of charge transport networks defined by an adjacency matrix with elements corresponding to intermolecular couplings. These intermolecular couplings are used as inputs into Fermi's Golden Rule to derive rate constants of hopping between sites in the morphology. Fermi's Golden Rule is used for comparison to our Kirchoff Index using the Adjacency Matrix definition of the absolute value of the electronic coupling because both terms ignore energetic disorder, and infer rate constants only from the magnitude of the intermolecular electronic coupling. In a system in which energetic disorder were considered, one would use a Marcus-Jortner-Levich type expression, and a definition of the adjacency matrix which incorporates energetic disorder.

Using these rates, a master equation between all sites in the system is established, and approximately solved using a kinetic monte carlo (KMC) approach. Simulations are run for 10 ns, and the location of the charge on the lattice is computed at the beginning and end of the trajectory. A cubic lattice containing 3,375 sites is used. A maximum coupling of 0.025 eV is allowed between nearest neighbor sites in our model, and these values vary continuously depending on the relative orientations of nearest neighbor molecules (again, see previous JPCL work for more details on the model).

Finally, the mean-squared hopping distance  $(\Delta r)^2$  can be related to the zero-field mobility or a diffusion constant via an Einstein-like relation. Consequently, comparison of the Kirchoff index of our example networks to the KMC derived  $(\Delta r)^2$  allows for a rigorous test of the relationship between the Kirchoff index and charge mobilities/diffusion constants. The results of these simulations are shown in Figure S7, where a clearly positive, monotonic relationship between charge mobility and the kirchoff index is observed for the 250 independently sampled morphologies, providing proof of the utility of the Kirchoff index as a qualitative metric of charge mobilities.



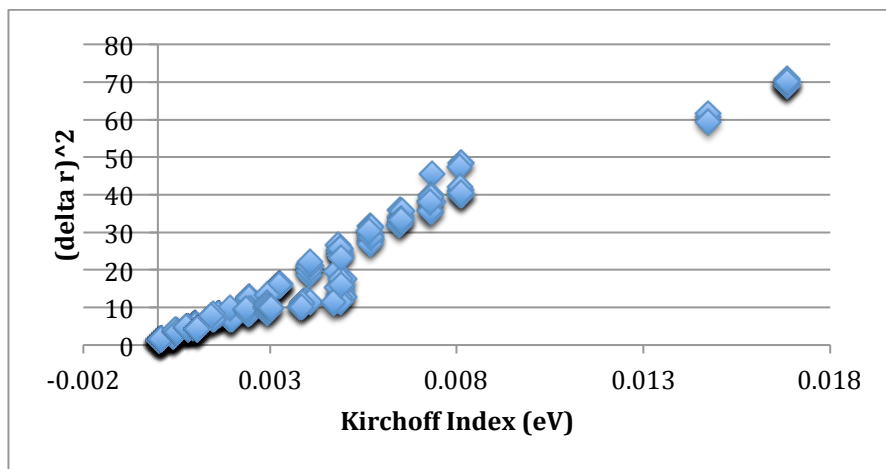


Figure S7 – Plot of KMC derived mean-squared displacement of charge vs network's Kirchoff Index. Units of  $\Delta r$  are in terms of lattice units.